J. Biochem. 124, 842-847 (1998)

Single-Step Purification and Characterization of MBP (Maltose Binding Protein)-DnaJ Fusion Protein and Its Utilization for Structure-Function Analysis

Yoshiyuki Ishii,* Syuji Sonezaki,* Yasushi Iwasaki,* Eiichi Tauchi,* Yoshikazu Shingu,* Koichi Okita,* Hiroaki I.-Ogawa,* Yasuhiko Kato,* and Akihiko Kondo†,1

*Department of Applied Chemistry, Faculty of Engineering, Kyushu Institute of Technology, Sensuicho, Tobata, Kitakyushu 804; and †Department of Chemical Science and Engineering, Faculty of Engineering, Kobe University, 1-1 Rokkodaicho, Nada, Kobe 657-8501

Received for publication, June 17, 1998

DnaJ is a molecular chaperone, which contains a zinc finger-like motif and cooperates with DnaK to mediate the folding of newly synthesized and denatured proteins. DnaJ was overproduced and purified using the maltose binding protein (MBP) fusion vector. The fusion protein (MBP-DnaJ) was expressed in a soluble form in *Escherichia coli* and purified to homogeneity using amylose resin in a single step. The UV-visible absorption spectrum of MBP-DnaJ showed peaks at 355 and 475 nm. Moreover, these absorption peaks disappeared upon treatment with ethylenediaminetetraacetic acid (EDTA) or *p*-hydroxymercuriphenylsulfonic acid (PMPS). Inductively coupled plasma (ICP) spectrometry demonstrated that MBP-DnaJ contains Fe ions as well as Zn ions. MBP-DnaJ mediated the replication of the λ phage *in vivo*, stimulated the ATPase activity of DnaK and prevented the aggregation of denatured rhodanase, indicating that fusion of MBP to the N-terminal of DnaJ does not affect the functions of DnaJ. To study the roles of bound metal ions, metal-free MBP-DnaJ, and MBP-DnaJ containing 2 Zn ions were prepared. MBP-DnaJ containing Fe and Zn ions, and MBP-DnaJ containing 2 Zn ions stimulated the ATPase activity of DnaK, prevented the aggregation of denatured rhodanase and bound to DNA to similar extents. On the other hand, metal-free MBP-DnaJ showed much lower DNA-binding ability and lower ability to prevent rhodanese aggregation. Therefore, the bound metal species do not affect the function of the zinc finger-like motif of DnaJ, whereas removal of the metal ions from DnaJ diminishes its binding ability as to DNA and denatured proteins.

Key words: DnaJ, DnaK, maltose binding protein, molecular chaperone, zinc finger-like motif.

When prokaryote and eukaryote cells are exposed to high temperature, the heat shock response occurs. The heat shock response results in the induction of so-called heat shock proteins, which mediate the proteolysis (*1*) and refolding (*2, 3*) of denatured proteins. Heat shock proteins, which mediate protein folding, also play important roles under physiological conditions (*4*) and are classified as molecular chaperones.

DnaJ protein, which is a molecular chaperone in *Escherichia coli*, was first identified as a host factor required for DNA replication of the λ phage (*5-8*). Subsequently, DnaJ has been shown to be involved in a variety of cellular processes, including DNA replication of the *E. coli* chromosome (*7*), P1 plasmid (*9*), and fertility factor F (*10*), protein folding (*11*) and protein translocation (*12*). DnaJ is known to function as a typical molecular chaperone in coordination with other heat shock proteins such as DnaK and GrpE (*11*). In the presence of DnaJ, the ATPase activity of DnaK is stimulated (*13, 14*) and the DnaK-substrate complex is stabilized (*15, 16*).

The various DnaJ homologs contain four conserved regions. The J-domain, which is the N-terminal 70-amino-acid-long region, is highly conserved and is responsible for stimulating the ATPase activity of DnaK (*17*). The tertiary structure of the J-domain has been demonstrated by NMR methodology (*18*). The G/F module, which is a 35-amino-acid-long region following the J-domain, is rich in both Gly and Phe amino acids. Deletion of the G/F module drastically interferes with DnaJ-dependent stabilization of DnaK-substrate complexes (*19*). The Cys-rich region, which is located downstream of the G/F module of some DnaJ-like proteins (*20*), contains four repeats of the sequence, Cys-X-X-Cys-X-Gly-X-Gly (*21, 22*), and resembles one of the zinc finger motifs. This region is also thought to be required for DnaJ to specifically bind to denatured proteins (*23*). The C-terminal region of all DnaJ-like proteins is much less conserved and could be responsible for substrate binding.

In the previous studies, purification of *E. coli* DnaJ was

[1] To whom correspondence should be addressed. Tel: +81-78-803-1147, Fax: +81-78-803-1171, E-mail: kondo@appchem.chme.kobe-u.ac.jp

started by solubilization of the pellet fraction with urea, and required several subsequent column chromatography steps (*23-25*). The purified DnaJ was found to bind two Zn ions through its zinc finger-like motif (*23, 25*). We describe the production of DnaJ carrying a maltose binding protein (MBP-DnaJ) at its N-terminal and its affinity purification from a soluble fraction of *E. coli* cells using amylose resin. The purified MBP-DnaJ was characterized, and used to study the interaction with DnaK, protein substrates, and single-stranded and double-stranded DNAs.

MATERIALS AND METHODS

Materials—*E. coli* strains DH5α and HMS174 were used. *E. coli* strains MC4100 (F′ *araD*Δ*(argF-lac)*U169 *rpsL relA flbB deoC ptsF rbsR*) and KY1456 (MC4100 *dnaJ*::Tn*10-42*) were gifts from Dr. Kitagawa (Nara Institute of Science and Technology, Nara). Plasmid pMAL-c2, encoding *malE* (Δ2-26) (MBP gene with deletion of the signal sequence), the pMAL primer and amylose resin were obtained from New England Biolabs (Beverly, MA, USA). Plasmids pUC118 and pUC119, restriction endonucleases, polymerase and ssM13 phage DNA were obtained from Takara Shuzo (Kyoto). Plasmids pT7-5 and pGP1-2 were gifts from Dr. Tabor (Department of Biological Chemistry and Molecular Pharmacology, the Harvard Medical School, USA) (*26*). Phage λ403, which contains the *dnaJ* gene, was obtained from the Kohara Gene Library Laboratory of the National Institute of Genetics, Mishima. Synthetic oligonucleotides were obtained from Funakoshi (Tokyo). *p*-Hydroxymercuriphenylsulfonic acid (PMPS) and rhodanase from bovine liver were obtained from Sigma Chemical (St. Louis, MO, USA). Ethylenediamine tetraacetic acid (EDTA), malachite green and ammonium molybdate were obtained from Nacalai Tesque (Kyoto). DnaK and GrpE from *E. coli* were obtained from Epicentra Technologies (Madison, WI, USA).

Plasmid Construction—The *dnaJ* gene from λ403 was subcloned between the *Eco*RI and *Bam*HI sites of pUC119 and pT7-5, the resultant plasmids being named pUC119dnaJ and pT7-5dnaJ, respectively.

The *dnaJ* gene was amplified by means of the standard polymerase chain reaction using the two primers, 5′-ATTTCAATGGCTAAGCAAGATTATTACGAG and 5′-CGCCACTCTAGAGGTGCTCGCATATCTTCAACG, which introduced a flanking *Xba*I site (underlined), with plasmid pUC119dnaJ as a template. After cleavage with *Xba*I, the resultant fragment was inserted into plasmid pMAL-c2 digested with *Xmn*I and *Eco*RI to yield plasmid pMAL-dnaJ. The DNA sequencing of pMAL-dnaJ was carried out by the dideoxy-chain-termination method with the pMAL primer.

Measurement of λvir Phage Growth In Vivo—MC4100 and KY1456 containing pMAL-c2 or pMAL-dnaJ were grown in LB medium at 30°C to a cell density of 2×10^8 cells/ml, centrifuged and then resuspended in 10 mM $MgSO_4$. The λ*vir* phage was added at a multiplicity of 0.1, and adsorption was allowed for 30 min at 37°C. After removing unadsorbed phage by centrifugation, the infected cells were diluted 100-fold with LB medium [Difco yeast extract (5 g/liter), Difco tryptone (10 g/liter), and NaCl (5 g/liter)] and then incubated for 3 h at 37°C, followed by the addition of several drops of chloroform. The layers were diluted and plated with MC4100, and then the phage titers were measured (*7*).

Protein Purification—DnaJ was purified from a pellet fraction of *E. coli* HMS174 cells containing plasmids pT7-5dnaJ and pGP1-2 as described by Zylicz *et al.* (*24*). The purified DnaJ was dialyzed against 20 mM Tris-HCl (pH 7.5), 200 mM NaCl, and 10% glycerol (buffer A), and then stored at −80°C.

MBP-DnaJ was purified from *E. coli* DH5α cells containing plasmid pMAL-dnaJ. Cultures of DH5α(pMAL-dnaJ) were grown at 37°C in 1 liter LB medium until $A_{660}=0.5$, and harvested after IPTG induction (final concentration, 0.3 mM) for 3 h. Cells were suspended in buffer A and then frozen at −80°C overnight. The frozen cells were thawed in an ice bath, and the sonicated cell suspension was centrifuged at $10{,}000\times g$ for 30 min. The supernatant was loaded onto amylose resin equilibrated with buffer A. Affinity purification of MBP-DnaJ using the amylose resin was performed as described by Riggs (*27*). Metal-free MBP-DnaJ [MBP-DnaJ(−)] was prepared by titration of MBP-DnaJ with PMPS followed by dialysis, and MBP-DnaJ(2 Zn), which contains two Zn ions, was prepared by the addition of DTT and $ZnCl_2$ to MBP-DnaJ(−), as described by Banecki *et al.* (*25*).

The protein concentration was determined by the Bradford method with bovine serum albumin as the standard. Sodium dodecyl sulfate polyacrylamide gel electrophoresis (SDS-PAGE) was performed as described by Garfin (*28*). A 15% polyacrylamide gel was used and stained with Coomassie Brilliant Blue R250.

Measurement of UV-Visible Absorption Spectra—UV-visible absorption spectra of 33.3 μM MBP-LacZα, 21.4 μM MBP-DnaJ, and 32.5 μM DnaJ in buffer A were measured with a U-best 30 spectrophotometer (JASCO). To measure the spectral change of MBP-DnaJ during EDTA treatment, 21.4 μM MBP-DnaJ was incubated in buffer A in the absence or presence of 100 mM EDTA at 37°C for 15 min. A PMPS titration experiment was performed as described by Banecki *et al.* (*25*). Five-microliters of 5 mM PMPS in buffer A was added to a 2 ml cuvette containing 4.35 μM MBP-DnaJ. The absorbance was measured at 250, 355, and 475 nm.

Measurement of Metal Contents—One hundred sixty-three micromolar MBP-DnaJ, 282 μM MBP-LacZ, or 67.9 μM hemoglobin in buffer A was diluted 30-fold with distilled water. The amounts of metals contained in these proteins (5.43 μM MBP-DnaJ, 9.40 μM MBP-LacZα, and 2.26 μM hemoglobin) were measured with a sequential plasma spectrometer ICPS-100TR (Shimadzu, Tokyo).

Measurement of ATPase Activity of DnaK—The ATPase activity of DnaK was measured by quantifying the inorganic phosphate produced during ATP hydrolysis by calorimetry as described by Mizobata *et al.* (*29*). DnaK (0.73 μM) and GrpE (1.5 μM) were incubated at 37°C in the presence of 1.5 μM DnaJ, MBP-DnaJ, MBP-DnaJ(−), MBP-DnaJ(2 Zn), or MBP-LacZα in 25 mM Hepes-KOH (pH 7.5), 100 mM KCl, and 10 mM $MgCl_2$ (buffer B) containing 2 mM ATP. Fifteen microliters samples were taken at the indicated times and mixed with 60 μl of 1 M perchoric acid. The samples were then mixed with a malachite green and ammonium molybdate solution, and then the absorbance at 660 nm was measured.

Measurement of Denatured Rhodanase Aggregation—

Aggregation of denatured bovine liver rhodanase was measured using a spectrophotometer as described by Langer *et al.* (*11*). Forty-six micromolar bovine liver rhodanase was denatured for 60 min at 25°C in 30 mM Tris-HCl (pH 7.4), 5 mM dithiothreitol (DTT), and 6 M guanidium-HCl (denaturation buffer). Twenty microliters of the denatured rhodanase was diluted in 2 ml of 10 mM Mopse-KOH (pH 7.2) and 50 mM KCl (buffer C) in the absence or presence of 0.92 and 2.3 μM DnaJ, MBP-DnaJ, MBP-DnaJ(−), MBP-DnaJ(2 Zn), or MBP-LacZα. Aggregation was measured with a spectrophotometer for 50 min at 25°C at the wavelength of 320 nm.

Interaction between DNAs and MBP-DnaJ, MBP-DnaJ(−), and MBP-DnaJ(2 Zn)—Twenty-five micrograms of MBP-DnaJ, MBP-DnaJ(−), MBP-DnaJ(2 Zn), or MBP-LacZα and 1.0 μg of ssM13 phage DNA or pUC118 plasmid DNA were incubated in 50 μl of buffer B for 10 min at 25°C. Forty microliters of amylose resin was added to the reaction mixture, which was then recovered by centrifugation at 5,000 rpm. The amylose resin was washed two times with 50 μl of buffer B. Protein-DNA complexes bound to the resin were then eluted with 30 μl of buffer B containing 10 mM maltose. DNA present in 20 μl of the eluted fraction was analyzed by 1% agarose gel electrophoresis.

RESULTS

λ Phage Growth in the dnaJ Mutant Containing Plasmid pMAL-dnaJ—DnaJ protein is necessary for λ phage replication. We examined whether or not MBP-DnaJ is capable of replicating the λ phage using a DnaJ mutant *E. coli* strain (Table I). The level of λ phage growth in KY1456(dnaJ$^-$) cells containing plasmid pMAL-DnaJ was similar to that in MC4100(dnaJ$^+$) cells, while the level of λ phage growth in KY1456(dnaJ$^-$) cells containing plasmid pMAL-c2 was very low. This indicates that MBP-DnaJ exhibits similar activity to wild type DnaJ *in vivo*.

Overproduction and Purification of MBP-DnaJ—Figure 1 shows SDS-PAGE analysis of the expression and purification of MBP-DnaJ. Plasmid pMAL-dnaJ gave a high level of expression of MBP-DnaJ (83 kDa, lane 2), and almost all of the fusion protein was detected in the soluble fraction (data not shown). Moreover, MBP-DnaJ was purified to homogeneity using amylose resin in a single step (lane 3). Forty-five milligrams of pure MBP-DnaJ was obtained from 1 liter of culture in shake flasks.

UV-Visible Absorption Spectrum of MBP-DnaJ—DnaJ, which was purified from the pellet fraction of *E. coli*, was colorless. However, MBP-DnaJ was a slightly red color. Figure 2 shows the UV-visible absorption spectra of DnaJ, MBP-DnaJ, and MBP-LacZα. The spectrum of DnaJ did not show any peak (dashed and dotted line). In contrast, the spectrum of MBP-DnaJ showed two peaks at 355 and 475 nm (solid line). Because the spectrum of MBP-LacZα did not show any peak (dashed line), the specific absorption peaks of MBP-DnaJ resulted from the DnaJ region. Moreover, these peaks of MBP-DnaJ completely disappeared on incubation with EDTA for 15 min at 37°C (data not shown), indicating that the DnaJ region contains divalent plus ions, which result in the specific absorption peaks.

UV-Visible Absorption Spectral Change of MBP-DnaJ during Titration with Mercurial Reagent PMPS—PMPS is known to release Zn ions from zinc-binding proteins (*25, 30*). The formation of a mercaptide bond between free Cys residues and PMPS can be monitored as the absorbance at 250 nm. Figure 3 shows that the absorbance at 250 nm increased on the addition of PMPS and reached a plateau at the ratio of 8 PMPS to each MBP-DnaJ monomer. In addition, the absorbance at 355 and 475 nm decreased and reached a plateau at the ratio of 8 PMPS to each MBP-DnaJ monomer, suggesting that 8 Cys residues are involved in the binding of metal ions. Metal ions, which give the absorption peaks at 355 and 475 nm, bind to Cys residues in the zinc finger-like motif of the DnaJ region of MBP-DnaJ.

Metal Ions Bound to MBP-DnaJ—In the previous studies, 4-(2-pyridylazo)resorcinol (PAR) analysis and

TABLE I. **λ phage growth in *dnaJ* mutant cells with and without pMAL-DnaJ.**

Strain	λ*vir* phage titer (pfu/ml)
MC4100(dnaJ$^+$)/pMAL-c2	2×10^{10}
MC4100(dnaJ$^+$)/pMAL-DnaJ	4×10^{10}
KY1456(dnaJ$^-$)/pMAL-c2	5×10^{4}
KY1456(dnaJ$^-$)/pMAL-DnaJ	2×10^{10}

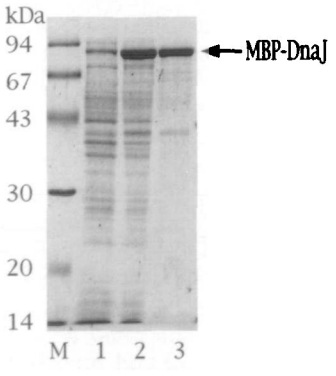

Fig. 1. **SDS-PAGE analysis (15% polyacrylamide gel) of crude and purified MBP-DnaJ.** A Coomassie Brilliant Blue R250 stained gel is shown. (M) Marker proteins, with sizes in kDa; (1) crude extract before IPTG induction (12.0 μg soluble fraction total protein); (2) crude extract after IPTG induction for 3 h (15.0 μg soluble fraction total protein); (3) affinity-purified MBP-DnaJ (3.0 μg total protein). The arrow indicates MBP-DnaJ.

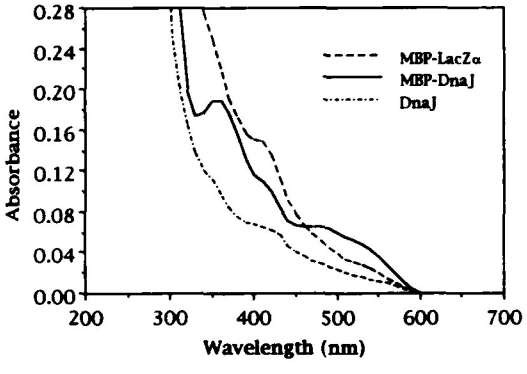

Fig. 2. **UV-visible absorption spectra of 33.3 μM MBP-LacZα.** (----), 21.4 μM MBP-DnaJ (——), and 32.5 μM DnaJ (– – –) in buffer A.

extended X-ray absorption fine structure (EXAFS) analysis showed that DnaJ purified from a pellet fraction of *E. coli* contains two zinc ions (*23, 25*). In this study, inductively coupled plasma (ICP) spectrometry was used to identify the metal ions which bind to MBP-DnaJ. Table II shows the molar ratios of metals to three proteins. Four Fe ions were detected for one hemoglobin molecule on ICP analysis, which is consistent with the previous result (*31*), indicating that ICP analysis is effective for determination of the ion species bound to proteins. On ICP analysis, the molar ratio of Fe/Zn/MBP-DnaJ was determined to be 0.9:0.9:1, whereas that of Fe/Zn/MBP-LacZα was determined to be 0.1:0.1:1.

Stimulation of ATPase Activity of DnaK by MBP-DnaJ—The ATPase activity of DnaK is known to be stimulated up to 50-fold in the presence of DnaJ and GrpE (*13, 14*). Figure 4 shows the enhancement of the ATPase activity of DnaK by DnaJ, MBP-DnaJ, MBP-DnaJ(−), MBP-DnaJ(2 Zn), or MBP-LacZα in the presence of GrpE. MBP-DnaJ, MBP-DnaJ(−), and MBP-DnaJ(2 Zn) stimulated the ATPase activity of DnaK to similar extents to DnaJ in the presence of GrpE. In contrast, the addition of MBP-LacZα did not affect the ATPase activity of DnaK. These results suggest that fusion of MBP to the N-terminal of DnaJ, the species of bound metal ions and the release of metal ions do not affect its ability to stimulate the ATPase activity of DnaK.

Suppression of Denatured Rhodanese Aggregation by MBP-DnaJ—DnaJ has been reported to bind to denatured rhodanese and to suppress its aggregation (*11*). Figure 5A shows the aggregation of rhodanese in the absence and presence of a twofold molar excess of DnaJ, MBP-DnaJ, MBP-DnaJ(−), or MBP-DnaJ(2 Zn). In the presence of DnaJ, rhodanese aggregation was significantly suppressed. This result is similar to the previous one (*11*). On the other hand, MBP-DnaJ and MBP-DnaJ(2 Zn) showed higher levels of suppression of the aggregation of rhodanese. In the presence of MBP-LacZα, aggregation was also suppressed (Fig. 5B), and the level of suppression of aggregation by MBP-LacZα was similar to that by MBP (data not shown). The higher levels of suppression of aggregation by these MBP-DnaJs compared with DnaJ are probably attributable to MBP. The level of suppression of aggregation by MBP-DnaJ(−) was lower compared with that by MBP-DnaJ and MBP-DnaJ(2 Zn), indicating that structure of the zinc finger-like motif affects its binding ability as to denatured proteins.

Interaction between DNAs, and MBP-DnaJ, MBP-DnaJ-(−), and MBP-DnaJ(2 Zn)—It has been suggested that DnaJ binds to ssM13 phage DNA (*24*). We tried to directly observe the interaction between MBP-DnaJ and ssM13 phage DNA or pUC118 plasmid DNA by using amylose resin. Figure 6 shows that MBP-DnaJ and MBP-DnaJ(2 Zn) bound to both ssM13 phage DNA and pUC118 plasmid DNA (lanes 2, 4, 7, and 9). In contrast, MBP-LacZα did not bind to these DNAs (lanes 5 and 10). Therefore, DnaJ binds to both single-stranded and double-stranded DNAs, and the metal species bound to DnaJ do not affect its DNA binding ability. On the other hand, the binding of DNA to MBP-DnaJ(−) was much weaker (lanes 3 and 8).

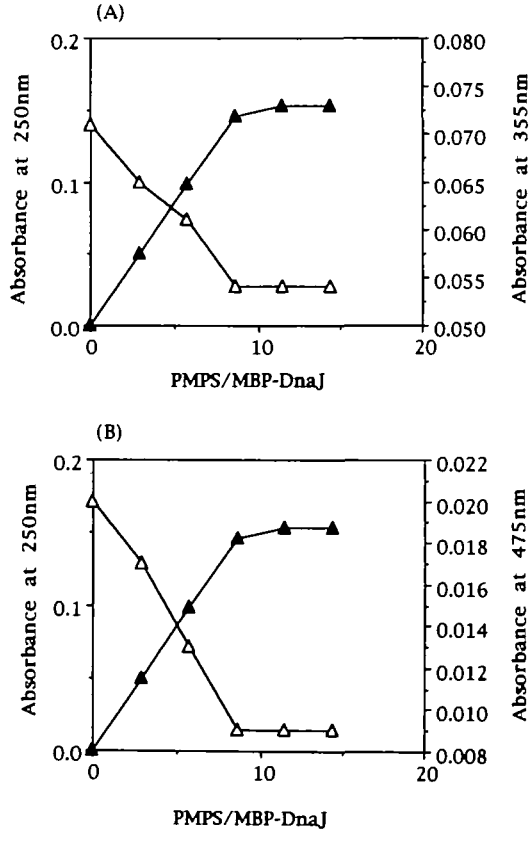

Fig. 3. **Spectral change of MBP-DnaJ during titration with the mercurial reagent, PMPS.** Various amounts of PMPS were added to 4.35 μM MBP-DnaJ. Absorbance was measured at 250 nm (panel A and B, ▲), 355 nm (panel A, △), and 475 nm (panel B, △).

TABLE II. **Molar amounts of metal ions contained in MBP-LacZα, MBP-DnaJ, and hemoglobin, as determined by ICP.**

Protein	Fe ion (mol/mol protein)	Zn ion (mol/mol protein)
MBP-LacZα	0.1	0.1
MBP-DnaJ	0.9	0.9
Hemoglobin	3.9	nt

nt, not tested.

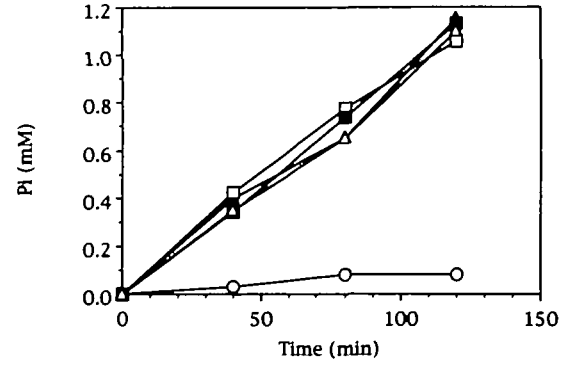

Fig. 4. **ATPase activity of DnaK.** The time course of ATP hydrolysis was determined by incubating 0.73 μM DnaK in buffer B containing 1.5 μM GrpE with 1.5 μM DnaJ (△), MBP-DnaJ (▲), MBP-DnaJ(−) (□), MBP-DnaJ(2 Zn) (■), or MBP-LacZα (○) at 37°C.

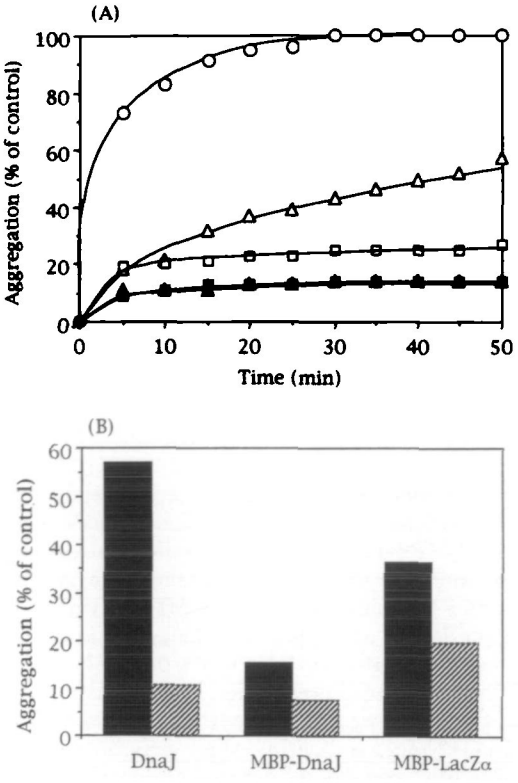

Fig. 5. **Suppression of rhodanese aggregation by DnaJ, MBP-DnaJ, MBP-DnaJ(−), MBP-DnaJ(2 Zn), and MBP-LacZα.** (A) Time course of aggregation of 0.46 μM denatured rhodanese in buffer C in the absence (○) or presence of 0.92 μM DnaJ (△), MBP-DnaJ (▲), MBP-DnaJ(−) (□), or MBP-DnaJ(2 Zn) (■) at 25°C. (B) Aggregation of 0.46 μM denatured rhodanese in buffer C in the presence of 0.92 μM (■) or 2.30 μM (▨) DnaJ, MBP-DnaJ, or MBP-LacZα after incubation at 25°C for 50 min.

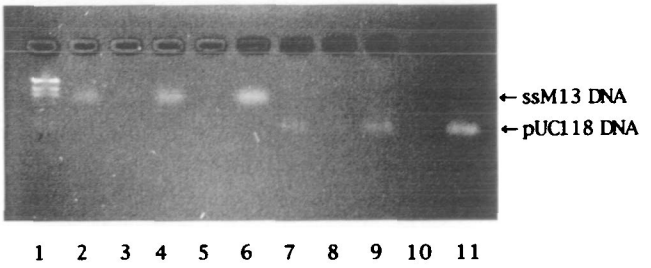

Fig. 6. **Interaction between DNA, and MBP-DnaJ, MBP-DnaJ-(−), and MBP-DnaJ(2 Zn).** MBP-DnaJ (lanes 2 and 7), MBP-DnaJ-(−) (lanes 3 and 8), MBP-DnaJ(2 Zn) (lanes 4 and 9), or MBP-*LacZα* (lanes 5 and 10) was incubated with ssM13 phage DNA (lanes 2–5) or pUC118 plasmid DNA (lanes 7–10), and subsequently mixed with amylose resin. The samples eluted from the amylose resin were analyzed by 1% agarose gel electrophoresis. (Lane 1) λ DNA digested with *Hin*dIII; (lane 6) ssM13 phage DNA; (lane 11) pUC118 plasmid DNA.

DISCUSSION

DnaJ has been shown to be involved in a variety of cellular processes, including DNA replication of the *E. coli* chromosome (*7*), P1 plasmid (*9*), and fertility factor F (*10*), protein folding (*11*) and protein translocation (*12*). From these effects, it is supposed that DnaJ functions in various locations in cells. However, DnaJ has been purified from the pellet fraction of *E. coli* cells. Moreover, its purification required many purification steps, such as urea solubilization, DEAE-Sephacel chromatography, ammonium sulfate precipitation, hydroxyapatite chromatography, and P-11-cellulose phosphate chromatography (*24*).

In this study, we propose the production of DnaJ as a MBP-DnaJ fusion protein. An *in vivo* λ phage growth experiment showed that MBP-DnaJ has a similar function to wild type DnaJ (Table I). MBP-DnaJ was affinity-purified from the soluble fraction of *E. coli* cells using amylose resin in a single step. The purified MBP-DnaJ was a slightly red color, and gave UV-visible absorption peaks at 355 and 475 nm (Fig. 2), although DnaJ, which was purified from the pellet fraction, was colorless. Moreover, these absorption peaks of MBP-DnaJ disappeared on EDTA or PMPS treatment. ICP analysis demonstrated that MBP-DnaJ contains Fe ions as well as Zn ions, and the molar ratio of Fe/Zn/MBP-DnaJ was approximately 1:1:1. These results suggest that MBP-DnaJ binds Fe ions as well as Zn ions through Cys residues in the zinc finger-like motif.

The rubredoxins from *Clostridium pasteurianum* and *Pseudomonas oleovorans* show a specific UV-visible absorption spectrum between 380 and 490 nm (*32- 34*). The rubredoxin from *C. pasteurianum* contains four Cys residues and one Fe ion, and that from *P. oleovorans* contains ten Cys residues and two Fe ions. These rubredoxins bind Fe ions through the four Cys residues of the two Cys-X-X-Cys sequences (*35-38*). The DnaJ protein also contains four repeats of the Cys-X-X-Cys sequence (*21, 22*). Zn and Fe ions probably bind to two Cys-X-X-Cys sequences, respectively in MBP-DnaJ from the soluble fraction, while two Zn ions were found to bind to four Cys-X-X-Cys sequences in DnaJ from the pellet fraction. Since the MBP affinity tag does not bind metal ions (Table II), the difference in metals in DnaJ and MBP-DnaJ probably results from their different localizations in *E. coli* cells. In addition, overexpressed MBP-DnaJ probably uses Fe ions as well as Zn ions because of the limited amounts of ions in the cells.

MBP-DnaJ containing Fe and Zn ions stimulated the ATPase activity of DnaK to a similar extent to DnaJ containing two Zn ions (Fig. 4). Moreover, MBP-DnaJ containing one Zn and one Fe ion showed similar ability to suppress the aggregation of denatured proteins to that containing two Zn ions (Fig. 5). Therefore, the bound ion species do not affect the function of DnaJ. On the other hand, metal-free MBP-DnaJ showed a lower level of suppression of rhodanese aggregation, although metal-free MBP-DnaJ stimulated the ATPase activity of DnaK to a similar extent to DnaJ. In the previous study, the zinc finger-like motif was found to be necessary for the recognition and binding of the denatured proteins, while the J-domain and the G/F module were found to be sufficient to stimulate the ATPase activity of DnaK (*23*). Our results are consistent with this observation. A correctly folded zinc finger-like motif is required for the DnaJ molecule to recognize and bind to denatured proteins.

It has been reported that DnaJ binds to ssM13 phage DNA (*24*). In this study, the interactions between DnaJ, and single-stranded and double-stranded DNAs were studied. MBP-DnaJ as well as MBP-DnaJ(2 Zn) was found to bind to single-stranded and double-stranded DNAs (Fig. 6). On the other hand, the binding of DNA to metal-free

MBP-DnaJ was much weaker. Therefore, two metal ions, which are tetrahedrally coordinated to four Cys residues, are required for the zinc finger-like motif of DnaJ to maintain the conformation for DNA binding.

In a previous study, Banecki *et al.* pointed out that bound metal ions play a role in stabilizing the tertiary structure of DnaJ (*25*). The above results indicate that metal ions are also necessary for the DnaJ function, although the species of metal ions does not affect its function.

We wish to thank Kenji Tatematu, Tadanaru Teshima and Akitoshi Sakaguti for their help in the experiments, and are also grateful to Stanley Tabor, Masanari Kitagawa, and Yuji Kohara for providing the plasmids, *E. coli* strains and phage.

REFERENCES

1. Sherman, M.Y. and Goldberg, A.L. (1992) Involvement of the chaperonin dnaK in the rapid degradation of a mutant protein in *Escherichia coli*. *EMBO J.* **11**, 71-77
2. Skowyra, D., Georgopoulos, C., and Zylicz, M. (1990) The *E. coli dnaK* gene product, the hsp70 homolog, can reactivate heat-inactivated RNA-polymerase in an ATP hydrolysis-dependent manner. *Cell* **62**, 939-944
3. Schroder, H., Langer, T., Hartl, F.U., and Bukau, B. (1993) DnaK, DnaJ and GrpE form a cellular chaperone machinery capable of repairing heat-induced protein damage. *EMBO J.* **12**, 4137-4144
4. Ellis, J. (1987) Proteins as molecular chaperones. *Nature* **328**, 378-379
5. Sunshine, M., Feiss, M., Stuart, J., and Yochem, J. (1977) A new host gene (*groPC*) necessary for lambda DNA replication. *Mol. Gen. Genet.* **151**, 27-34
6. Saito, H. and Uchida, H. (1977) Initiation of the DNA replication of bacteriophage lambda in *Escherichia coli* K12. *J. Mol. Biol.* **113**, 1-25
7. Saito, H. and Uchida, H. (1978) Organization and expression of the *dnaJ* and *dnaK* genes of *Escherichia coli* K12. *Mol. Gen. Genet.* **164**, 1-8
8. Yochem, J., Uchida, H., Sunshine, M., Saito, H., Georgopoulos, C.P., and Feiss, M. (1978) Genetic analysis of two genes, *dnaJ* and *dnaK*, necessary for *Escherichia coli* and bacteriophage lambda DNA replication. *Mol. Gen. Genet.* **164**, 9-14
9. Tilly, K. and Yarmolinsky, M. (1989) Participation of *Escherichia coli* heat shock proteins DnaJ, DnaK and GrpE in P1 plasmid replication. *J. Bacteriol.* **171**, 6025-6029
10. Kawasaki, Y., Wada, C., and Yura, T. (1990) Roles of *Escherichia coli* heat shock proteins DnaK, DnaJ and GrpE in mini-F plasmid replication. *Mol. Gen. Genet.* **220**, 277-282
11. Langer, T., Lu, C., Echols, H., Flanagan, J., Hayer, M.K., and Hartl, F.U. (1992) Successive action of DnaK, DnaJ and GroEL along the pathway of chaperone-mediated protein folding. *Nature* **356**, 683-689
12. Wild, J., Altman, E., Yura, T., and Gross, C.A. (1992) DnaK and DnaJ heat shock proteins participate in protein export in *Escherichia coli*. *Genes Dev.* **6**, 1165-1172
13. Liberek, K., Marszalek, J., Ang, D., Georgopoulos, C., and Zylic, M. (1991) *Escherichia coli* DnaJ and GrpE heat shock proteins jointly stimulate ATPase activity of DnaK. *Proc. Natl. Acad. Sci. USA* **88**, 2874-2878
14. Szabo, A., Langer, T., Schroder, H., Flanagan, J., Bukau, B., and Hartl, F.U. (1994) The ATP hydrolysis-dependent reaction cycle of the *Escherichia coli* Hsp70 system-DnaK, DnaJ, and GrpE. *Proc. Natl. Acad. Sci. USA* **91**, 10345-10349
15. Wawrzynow, A., Banecki, B., Wall, D., Liberek, K., Georgopoulos, C., and Zylicz, M. (1995) ATP hydrolysis is required for the DnaJ-dependent activation of DnaK chaperone for binding to both native and denatured protein substrates. *J. Biol. Chem.* **270**, 19307-19311
16. Wawrzynow, A. and Zylicz, M. (1995) Divergent effects of ATP on the binding of the DnaK and DnaJ chaperones to each other, or to their various native and denatured protein substrates. *J. Biol. Chem.* **270**, 19300-19306
17. Wall, D., Zylicz, M., and Georgopoulos, C. (1994) The NH_2-terminal 108 amino acids of the *Escherichia coli* DnaJ protein stimulate the ATPase activity of DnaK and are sufficient for λ replication. *J. Biol. Chem.* **269**, 5446-5451
18. Szyperski, T., Pellechia, M., Wall, D., Georgopoulos, C., and Wuthrich, K. (1994) NMR structure determination of the *Escherichia coli* DnaJ molecular chaperone: secondary structure and backbone fold of the N-terminal region (residues 2-108) containing the highly conserved J domain. *Proc. Natl. Acad. Sci. USA* **91**, 11343-11347
19. Wall, D., Zylicz, M., and Georgopoulos, C. (1995) The conserved G/F motif of the DnaJ chaperone is necessary for the activation of the substrate binding properties of the DnaK chaperone. *J. Biol. Chem.* **270**, 2139-2144
20. Caplan, A.J., Cyr, D.M., and Douglas, M.G. (1993) Eukaryotic homologues of *Escherichia coli dnaJ*: a diverse protein family that functions with hsp70 stress proteins. *Mol. Biol. Cell* **4**, 555-563
21. Bardwell, J.C.A., Tilly, K., Craig, E., King, J., Zylicz, M., and Georgopoulos, C. (1986) The nucleotide sequence of the *Escherichia coli* K12 *dnaJ*$^+$ gene. A gene that encodes a heat shock protein. *J. Biol. Chem.* **261**, 1782-1785
22. Ohki, M., Tamura, F., Nishimura, S., and Uchida, H. (1986) Nucleotide sequence of the *Escherichia coli dnaJ* gene and purification of the gene product. *J. Biol. Chem.* **261**, 1778-1781
23. Szabo, A., Korszun, R., Hartl, F.U., and Flanagan, J. (1996) A zinc finger-like domain of the molecular chaperone DnaJ is involved in binding to denatured protein substrates. *EMBO J.* **15**, 408-417
24. Zylicz, M., Yamamoto, T., McKittrick, N., Sell, S., and Georgopoulos, C. (1985) Purification and properties of the dnaJ replication protein of *Escherichia coli*. *J. Biol. Chem.* **260**, 7591-7598
25. Banecki, B., Liberek, K., Wall, D., Wawrzynow, A., Georgopoulos, C., Bertoli, E., Tanfani, F., and Zylicz, M. (1996) Structure-function analysis of the zinc finger region of the DnaJ molecular chaperone. *J. Biol. Chem.* **271**, 14840-14848
26. Tabor, S. and Richardson, C.C. (1985) A bacteriophage T7 RNA polymerase/promoter system for controlled exclusive expression of specific genes. *Proc. Natl. Acad. Sci. USA* **82**, 1074-1078
27. Riggs, P. (1992) Expression and purification of maltose binding protein fusion in *Short Protocols in Molecular Biology*, 2nd ed. (Ausubel, F.M., Brent, R., Kingston, R.E., Moore, D.D., Seidman, J.G., Smith, J.A., and Struhl, K., eds.) pp. 16.21-16.27, Green Publishing Associates, and John Wiley and Sons, New York
28. Garfin, D.E. (1990) One-dimensional gel electrophoresis. *Methods Enzymol.* **182**, 425-441
29. Mizobata, T., Akiyama, Y., Ito, K., Yumoto, N., and Kawata, Y. (1992) Effects of the chaperonin GroE on the refolding of tryptophanase from *Escherichia coli*. Refolding is enhanced in the presence of ADP. *J. Biol. Chem.* **267**, 17773-17779
30. Hunt, J.B., Neece, S.H., and Schachman, H.K. (1984) A. Ginsburg, Mercurial-promoted Zn^{2+} release from *Escherichia coli* aspartate transcarbamoylase. *J. Biol. Chem.* **259**, 14793-14803
31. Fasman, G.D., ed. (1976) *Handbook of Biochemistry and Molecular Biology, Protein*, Vol. 3, CRC Press, Cleveland
32. Lovenberg, W. and Sobel, B.E. (1965) Rubredoxin; A new electron transfer protein from *Clostridium pasteurianum*. *Proc. Natl. Acad. Sci. USA* **54**, 193-199
33. Peterson, J.A. and Coon, M.J. (1968) Enzymatic ω-oxidation. *J. Biol. Chem.* **243**, 329-334
34. Lode, E.T. and Coon, M.J. (1971) Enzymatic ω-oxidation. *J. Biol. Chem.* **246**, 791-802
35. Herriott, J.R., Sieker, L.C., Jensen, L.H., and Lovenberg, W. (1970) Structure of rubredoxin: An X-ray study to 2.5 Å resolution. *J. Mol. Biol.* **50**, 391-406
36. Watenpaugh, K.D., Sieker, L.C., and Jensen, L.H. (1979) The structure of rubredoxin at 1.2 Å resolution. *J. Mol. Biol.* **131**, 509-522
37. Watenpaugh, K.D., Sieker, L.C., and Jensen, L.H. (1980) Crystallographic refinement of rubredoxin at 1.2 Å resolution. *J. Mol. Biol.* **138**, 615-633
38. Adman, E.T., Sieker, L.C., Jensen, L.H., Bruschi, M., and LeGall, J. (1977) A structural model of rubredoxin from *Desulfovibrio vulgaris* at 2 Å resolution. *J. Mol. Biol.* **112**, 113-120